CHEMISTRY OF MATERIALS

pubs.acs.org/cm Article

Selective Capture of Ba^{2+}, Ni^{2+}, and Co^{2+} by a Robust Layered Metal Sulfide

Yu-Jie Gao, Hai-Yan Sun, Ji-Long Li, Xing-Hui Qi, Ke-Zhao Du, Yi-Yu Liao, Xiao-Ying Huang, Mei-Ling Feng,* and Mercouri G. Kanatzidis*

Cite This: *Chem. Mater.* 2020, 32, 1957−1963 Read Online

ACCESS | Metrics & More | Article Recommendations | Supporting Information

ABSTRACT: ^{133}Ba, ^{63}Ni, and ^{60}Co are hazardous to the ecosystem and human health. Their nonradioactive isotopes are also worthy of concern as toxic metal ions. Barium can be studied as a simulant of hazardous ^{226}Ra because of their comparable ionic radii and similar ion exchange behaviors. Herein, we report that the layered metal sulfide $(Me_2NH_2)_{1.33}(Me_3NH)_{0.67}Sn_3S_7{\cdot}1.25H_2O$ (FJSM-SnS) exhibits excellent capture properties for Ba^{2+}, Ni^{2+}, and Co^{2+} with high capacities (q_m^{Ba} = 289.0 mg/g; q_m^{Ni} = 83.27 mg/g; and q_m^{Co} = 51.98 mg/g), fast kinetics (within 5 min), wide pH durability, and outstanding Ba^{2+} selectivity. FJSM-SnS exhibits high removal efficiencies (>99%) for these ions in ion-exchange column experiments. The material possesses radiation resistance with good structural and crystal stability; it survives highly acidic conditions. Our results point to a promising scavenger for Ba^{2+}, Ni^{2+}, and Co^{2+} and, by extension, the even more harmful ^{226}Ra, which suggest that metal sulfide materials should be considered as effective scavengers for these ions from complex wastewater.

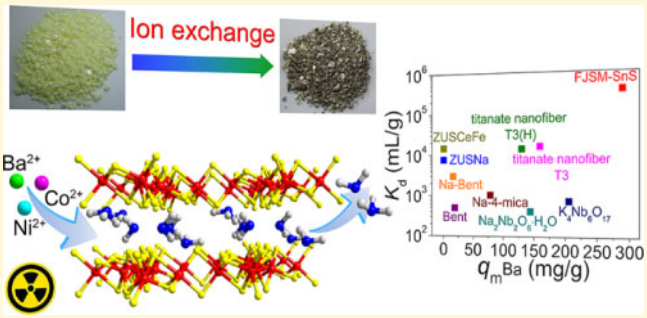

INTRODUCTION

Radioactive contaminants are generated from mine tailings, spent nuclear fuel reprocessing, nuclear accidents, and radioactive products used in industry, agriculture, medicine, and academia.[1−4] Liquid radioactive wastes are of particular concern because of their extremely harmful effects on humans and the environment. Barium, for example, has many radioactive isotopes. Among them, ^{133}Ba with a relatively long half-life ($T_{1/2} \approx 10.7$ y) exists in the byproduct of nuclear fuel fissions and emits γ ray at an energy of 356 keV.[5,6] Moreover, it is well known that soluble salts of nonradioactive Ba^{2+} are harmful to animals, plants, and humans.[7−10] The maximum permissible concentration of nonradioactive Ba^{2+} in drinking water documented by the U.S. Environmental protection agency (EPA) is 2 mg/L, while the WHO's limit is only 0.7 mg/L.[11−13] Barium pollution, however, has been getting more attention.[11,12,14−22] Importantly, it has been documented that barium can be studied as a simulant of hazardous ^{226}Ra because of their comparable ionic radii (1.34 Å for Ba^{2+} and 1.43 Å for Ra^{2+}) and similar ion exchange behaviors.[11,14,15,18,21,22] ^{226}Ra can generate a large radiation dose for an extremely long period of time (γ emitter with a half-life of 1600 ± 7 y) and decays into harmful ^{222}Rn gas. ^{226}Ra as the daughter radionuclide of ^{238}U, which constitutes the main radioactive waste in uranium mill tailings, is known to possess high mobility in the geosphere and can enter the food chain.[5,18,23,24]

The ^{60}Co ($T_{1/2} \approx 5.3$ y) isotope emits strong γ radiation, ^{63}Ni ($T_{1/2} \approx 100.1$ y) emits pure β radiation, and both can be derived from neutron activation of reactor materials.[25−27] Both ^{60}Co and ^{63}Ni can be released from the pressurized water nuclear power reactors even under normal operating conditions.[25,28] For instance, liquid wastes including ^{60}Co and ^{63}Ni from French nuclear facilities entered the freshwater related to the River Rhône.[29] Nonradioactive Co and Ni ions are widely applied in medicine, academia, and industry including electroplating, smelting, and battery manufacturing.[30,31] They are considered toxic to the ecosystem and human health.[30] The tolerance limit for Co(II) in potable water is 0.05 mg/L,[32] while the WHO's limit for Ni(II) is 0.07 mg/L.[13]

Eliminating barium, cobalt, and nickel from complex wastewater is therefore important, and several approaches have been used to remove Ba^{2+}, Ni^{2+}, and Co^{2+} from wastewater including precipitation, solvent extraction, adsorption, and ion exchange.[33−36] The ion exchangers investigated for Ba^{2+} removal are mostly oxide materials such as

Received: November 21, 2019
Revised: January 21, 2020
Published: January 23, 2020

https://dx.doi.org/10.1021/acs.chemmater.9b04831
Chem. Mater. 2020, 32, 1957−1963

zeolites,[11,14,20,21] clays,[11,17] modified zeolites,[22] modified clays,[15,17] titanate nanofibers,[16] and niobates.[18,19] However, they suffer from low capacity and poor selectivity. The sorbent materials for Ni^{2+} and Co^{2+} removal are generally zeolites,[37] clays,[33,38] and activated carbon,[39,40] which show low selectivity and fail to remediate solutions at low ion concentrations. On the other hand, selective uptake of radioactive ions presents a serious challenge because of the additional complexity of these liquid wastes. For instance, high-concentration Na^+ and other ions are always present in nuclear waste liquids.[41] Therefore, there is sufficient motivation to develop more effective ion exchangers that could selectively remove barium, nickel, and cobalt from a wide variety of wastewater systems.

Recently, metal sulfide ion-exchangers have proven promising as new materials that can achieve high performance in removing heavy metal ions such as Hg^{2+} and Pb^{2+} and radioactive ions of UO_2^{2+}, $^{137}Cs^+$, and $^{90}Sr^{2+}$.[42−49,58] Owing to their soft Lewis basic character, metal sulfides offer a unique function that is not available in the conventional oxide materials, namely, strong innate binding affinity for softer Lewis acidic metal ions. However, studies of metal sulfide ion-exchangers for removing radioactive Ba^{2+}, Co^{2+}, and Ni^{2+} are still in their infancy.[35,42,50−53] Herein, we report the efficient and selective capture of Ba^{2+}, Ni^{2+}, and Co^{2+} ions with an acid- and radiation-resistant layered metal sulfide $(Me_2NH_2)_{1.33}(Me_3NH)_{0.67}$-$Sn_3S_7$·$1.25H_2O$ (FJSM-SnS). Ba^{2+} is generally considered a hard Lewis acid cation, albeit within the alkaline earth group of ions, it is the softest. Ni^{2+} and Co^{2+} on the other hand are viewed as borderline soft Lewis acids. In this study, we found that Ba^{2+}, Ni^{2+}, or Co^{2+} are sufficiently soft for FJSM-SnS to exhibit high selectivities. It does so with high capacities, fast kinetics, and wide pH durability, while achieving very low residual concentrations for Ba^{2+}, Ni^{2+}, and Co^{2+}. Moreover, the material possesses radiation resistance with good structural and crystal stability; it survives highly acidic conditions. With these advantages, facile synthesis and environmentally friendly nature, FJSM-SnS is a promising scavenger for Ba^{2+}, Ni^{2+}, and Co^{2+} and, by extension, the even more harmful ^{226}Ra.

EXPERIMENTAL SECTION

Materials and Synthesis. $SnCl_4$·$5H_2O$ (98%, Sigma-Aldrich), sulfur sublimed (99.5%, Chengdu Kelong Chemical Co. Ltd.), and dimethylamine solution (40% in water, Shanghai Mackiln Biochemical Co. Ltd.) were used without further purification. A mixture of $SnCl_4$·$5H_2O$, sublimed sulfur, dimethylamine solution, and water was sealed in a stainless steel reactor with a Teflon liner, heated at 180 °C for 7 days, and cooled to room temperature, as we previously reported.[47] The obtained solid product was yellow hexagonal bulk crystals mixed with yellow powder both of which were shown to be FJSM-SnS by powder X-ray diffraction (PXRD). Ground polycrystalline samples of FJSM-SnS were utilized in batch ion-exchange experiments. Samples composed of larger particles of FJSM-SnS (on the scale of a few millimeters) were used to fill the ion-exchange column to avoid the loss of material during the column experiments.

Physical Measurements and Irradiation Studies. Scanning electron microscope (SEM) analysis was carried out on a JEOL JSM-6700F scanning electron microscope. Energy-dispersive spectroscopy (EDS) was measured using a HITACHI FE-SEM SU8010. PXRD patterns were collected in the angular range of 2θ = 5−65° at room temperature on a Miniflex II diffractometer with Cu Kα (λ = 1.54178 Å), a Bruker D8 Advance diffractometer with Cu Kα radiation (λ = 1.5418 Å), and a Lynxeye one-dimensional detector. FJSM-SnS samples were irradiated at a dose rate of 1.2 kGy/h with three different doses of 20, 100, and 200 kGy in the ^{60}Co γ irradiation experiments and at a dose rate of 20 kGy/h with three different doses of 20, 100, and 200 kGy in β irradiation experiments. The γ-ray irradiation was provided by a ^{60}Co irradiation source (92.42 PBq) in Suzhou CNNC Huadong Radiation Co., Ltd, China. The β irradiation was conducted using electron beams (10 MeV) provided by an electron accelerator located in CGN Dasheng Electron Accelerator Co., Ltd in Jiangsu Province of China.

X-ray photoelectron spectroscopy (XPS) was performed using an ESCALAB 250Xi X-ray photoelectron spectrometer microprobe. The inductively coupled plasma−optical emission spectroscopy (ICP−OES) and the inductively coupled plasma−mass spectroscopy (ICP−MS) were performed on a Thermo 7400 and a XSerise II, respectively.

Ion-Exchange Experiments. Considering the high toxicity of ^{133}Ba, ^{63}Ni, and ^{60}Co, their nonradioactive isotopes were used in the ion exchange experiments and the typical ion-exchange experiments of FJSM-SnS with ACl_2 (A = Ba^{2+}, Ni^{2+}, and Co^{2+}) are as follows. All the experiments were conducted at ∼25 °C using the batch sorption method. Ground polycrystalline powders of FJSM-SnS (10 mg) were added to aqueous solutions of ACl_2 with different concentrations of Ba^{2+}, Ni^{2+}, or Co^{2+} (10 mL). Then, the mixture was kept under magnetic stirring at ∼25 °C. After treatment, the yellow polycrystalline material was separated by filtration using a 0.22 μm Millipore filter on a 10 mL syringe and washed several times with ethanol, leaving a clear supernatant. The concentrations of Ba^{2+}, Ni^{2+}, and Co^{2+} in the clear supernatant were determined by ICP−OES or ICP−MS. These solutions were diluted with ultrapure water to meet the concentration range of the test instrument.

Isotherm Experiments. Solutions of Ba^{2+}, Ni^{2+}, and Co^{2+} with different concentrations were prepared, and the ratio of V/m of 1000 mL/g (V = 10 mL, m = 10 mg) was used for all cases. After 24 h, the filtered suspensions were analyzed with ICP−OES (Tables S1−S3).

Kinetics Experiments of Ion-Exchange. Ion-exchange experiments were performed for various reaction times. An amount of 100 mg of FJSM-SnS polycrystalline powders was added into a 100 mL solution containing ∼370 μg/L of barium ions, which is comparable to the actual concentration of barium contaminants found in groundwater samples.[54] The concentrations of the Ni and Co ions were ∼1100 μg/L. The solution mixtures were magnetically stirred for various reaction times, and the filtered solutions were analyzed by ICP−MS (Tables S5−S7).

pH-Dependent Ion-Exchange Experiments. The solutions of Ba^{2+} were prepared with different pH (3.3−10.8) values with concentrations varying from 264.4 to 857.8 μg/L (Table S8). The solutions of Ni^{2+} and Co^{2+} with different pH (2.3−10.8) were prepared with initial concentrations varying from 835 to 1147 μg/L (Table S9). The pH was regulated by NaOH or HCl solutions. The ion-exchange lasted ∼24 h at ∼25 °C, and the V/m of all the samples was 1000 mL/g (V = 30 mL, m = 30 mg). Then, the filtered solutions were analyzed with ICP−MS.

Ion-Exchange Experiments with Samples before and after Irradiation. The pristine unirradiated FJSM-SnS and its samples after 200 kGy β irradiation and 200 kGy γ irradiation were added to mixed solutions of Ba^{2+}, Ni^{2+}, and Co^{2+} (Table S10). The ion-exchange was performed as above. Then, the concentrations of Ba^{2+}, Ni^{2+}, and Co^{2+} and potential leaching of Sn^{4+} were analyzed with ICP−MS.

Competitive Ion-Exchange Experiments. The ion-exchange experiments with FJSM-SnS were carried out at the V/m ratio of 1000 mL/g, ∼25 °C and 24 h contact time. We used different conditions, such as in the presence of individual alkali or alkaline-earth metal ions (K^+, Cs^+, Ca^{2+}, and Mg^{2+}, Table S11), in the presence of Na^+ (Na^+:Ba^{2+} molar ratios in the range of 14.37−23 219, Table S12), and in the simulated groundwater (Table S13). We also tested FJSM-SnS with solutions of Cs^+, Sr^{2+}, UO_2^{2+}, Eu^{3+}, Ba^{2+}, Ni^{2+}, and Co^{2+} (Tables S14 and S15). Finally, we also performed Ba^{2+} ion exchange experiments in the presence of individual solutions of Pb^{2+}, Mn^{2+}, and Fe^{3+} as the competitive ions using V/m ratio of 1000 mL/g, ∼25 °C and 1 h contact time (Tables S16).

Elution Experiments. The Ba^{2+}, Ni^{2+}, and Co^{2+}-exchanged products of FJSM-SnS were used for elution experiments. An amount of ∼20 mg was added to 20 mL 0.5 M KCl solutions and stirred for

https://dx.doi.org/10.1021/acs.chemmater.9b04831
Chem. Mater. 2020, 32, 1957−1963

12 h at ~25 °C. After this treatment, the solid samples were analyzed by the EDS, elemental distribution mapping, and PXRD.

Ion-Exchange Column Experiments. A glass column was filled with ~3.1 g of FJSM-SnS using particles of a few millimeters. The inside diameter of the column was 13.4 mm, and a small amount of medical purified cotton was placed at the bottom of the column to avoid material loss (Figure S1). The solution slowly passed through the column by gravity. A typical ion-exchange experiment of FJSM-SnS with Ba^{2+}, Ni^{2+}, and Co^{2+} ions was as follows: Initially, fifty bed volumes of the solution (140 mL) slowly passed through the column and were collected at the bottom in a 200 mL serum bottle, and the solutions were analyzed. Then, a similar number of bed volumes slowly passed through the same column, and finally, 1100 bed volume solution (3.08 L) were passed and the solutions were analyzed. The initial ion concentrations were in the range of 704.9–928.6 μg/L, and the final concentrations in the outlet solution are shown in Table S17.

RESULTS AND DISCUSSION

Structure and Stability of FJSM-SnS. Multigram-scale samples of FJSM-SnS were synthesized through a one-pot solvothermal route. Single crystal X-ray crystallography[47] shows that the material features a layered structure of $[Sn_3S_7]_n^{2n-}$, consisting of edge-sharing $[Sn_3S_4]$ clusters that form a perforated layer (Figure 1a). The layers are separated by $[Me_2NH_2]^+$ and $[Me_3NH]^+$ cations (Figure 1b).

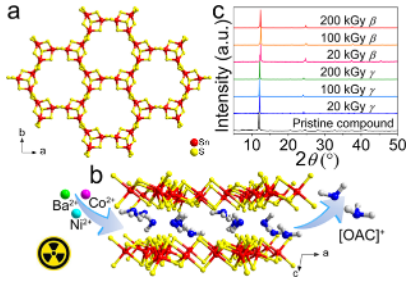

Figure 1. (a) $[Sn_3S_7]_n^{2n-}$ layer in FJSM-SnS; (b) arrangement of two adjacent layers and the organic ammonium cations (C, gray; N, blue; and $[OAC]^+$ = $[Me_2NH_2]^+$ and $[Me_3NH]^+$) located in the interlayer space; guest water molecules are omitted for clarity; (c) PXRD patterns of pristine FJSM-SnS and the samples after β and γ irradiations.

The success of a sorbent designed for removing radioactive ions depends in part on its ability to be acid and radiation resistant. In this context, we subjected FJSM-SnS to radiation exposure and as an initial assessment found it to be structurally radiation resistant. Specifically, FJSM-SnS samples were irradiated at a dose rate of 1.2 kGy/h for three different doses of 20, 100, and 200 kGy using ^{60}Co γ radiation experiments. We also used a dose rate of 20 kGy/h for three different doses of 20, 100, and 200 kGy in β irradiation experiments. The samples exhibited no structural and crystal degradation even under 200 kGy β (10 MeV) or 200 kGy of ^{60}Co γ ray irradiation, as suggested by PXRD (Figure 1c). Of course, far more systematic experiments will be required to make a full assessment of this type of stability, but such work is outside of the scope of this report.

In addition, we also assessed the stability of FJSM-SnS in acid solutions. Based on PXRD, the material retains its layered structure down to pH ~ 0.6 (Figure S20). Furthermore, the concentrations of dissolved Sn for FJSM-SnS soaked in acid solutions were in the range of 45.9–671.90 μg/L, corresponding to very low dissolution rates of Sn, that is, 0.009% at pH = 3.6–0.133% at pH = 0.6 (Table S21 and Figure S21). Generally, sulfides were considered to be unstable in acidic solutions. The acid and radiation resistance of FJSM-SnS are therefore additional advantages for the material when considering it for removing radionuclides in practice.

Characterization of Ion-Exchanged Products. The exchange of $[OAC]^+$ in FJSM-SnS with Ba^{2+}, Ni^{2+}, and Co^{2+} were confirmed by a wide variety of physical methods including inductively coupled plasma spectroscopy (ICP), PXRD patterns, EDS, and XPS. PXRD shows that Ba^{2+}, Ni^{2+}, and Co^{2+} ion exchanged products are isostructural with the pristine compound, and the interlayer distances decrease after ion exchange as revealed by the shifting of (002) Bragg peaks to higher 2θ (lower d spacing) (Figure S2). EDS analyses of the ion-exchanged samples show that Ba^{2+}, Ni^{2+}, and Co^{2+} ions entered the crystallites (Figures S3–S5). Elemental distribution mapping reveals the presence of the captured Ba^{2+}, Ni^{2+}, and Co^{2+} ions and their homogeneous distributions in the samples (Figure S6). XPS of the exchanged products show the presence of characteristic peaks of Ba 3d, Ni 2p, and Co 2p, which further confirms the success of Ba^{2+}, Ni^{2+}, and Co^{2+} ion exchange, respectively (Figure S7).

Adsorption Isotherm Studies. The adsorption isotherms of FJSM-SnS for Ba^{2+}, Ni^{2+}, and Co^{2+} are shown in Figure 2.

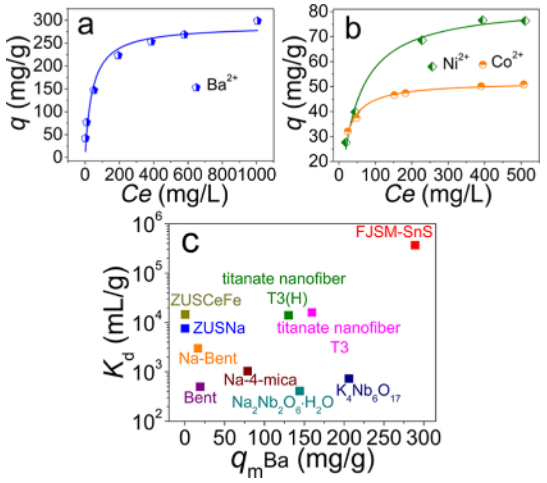

Figure 2. (a) Ba^{2+} ion-exchange isotherm for FJSM-SnS; (b) Ni^{2+} and Co^{2+} ion-exchange isotherms for FJSM-SnS; (c) comparison of Ba^{2+} removal capacity and the K_d value for FJSM-SnS with those of other materials: titanate nanofiber T3(H) and titanate nanofiber T3,[16] $Na_2Nb_2O_6{\cdot}H_2O$,[19] $K_4Nb_6O_{17}$,[18] and Na-4-mica (the K_d value was measured by removing Ra^{2+}, which is the analogue of Ba^{2+}),[15] ZUSCeFe and ZUSNa,[22] Na-Bent and Bent;[17] the maximum uptake capacity q_m^{Ba} of 289.0 ± 15.91 mg/g and K_d^{Ba} value of 3.68×10^5 mL/g for FJSM-SnS under excess and competitive Ca^{2+} are shown.

Figure 2a, b plots the capacities for Ba^{2+}, Ni^{2+}, and Co^{2+}-exchange against the concentration at equilibrium. The Langmuir models could well fit the equilibrium isotherms, yielding R^2 values of 0.953, 0.990, and 0.987 for Ba^{2+}, Ni^{2+}, and Co^{2+}, respectively. The Langmuir model is based on the assumption that adsorption occurs on a homogeneous surface and a maximum uptake exists. It is also assumed that all the adsorption sites have the same sorption activation energy (and thus constant and independent of surface coverage) and there is no transmigration of adsorbate from one site to another.[55] It is described by eq 1.

https://dx.doi.org/10.1021/acs.chemmater.9b04831
Chem. Mater. 2020, 32, 1957–1963

$$q = q_m \frac{bC_e}{1 + bC_e} \quad (1)$$

Here, q (mg/g) is the exchange capacity at the equilibrium concentration C_e (mg/L), which can be calculated from eq 2; q_m represents the maximum exchange capacity, and b (L/mg) is the Langmuir constant related to the energy of the adsorption.

$$q = \frac{(C_0 - C_e)V}{m} \quad (2)$$

where C_0 and C_e (mg/L) are the initial and equilibrium concentrations, respectively. V (mL) and m (g) are the volume of the solution and the amount of the ion-exchanger used in the ion-exchange experiment, respectively.

The corresponding parameters of the fitting results are shown in Table S4. It is noteworthy that the maximum uptake capacity q_m^{Ba} by FJSM-SnS is 289.0 ± 15.91 mg/g (Table S4), which is higher than those of the most previously reported Ba^{2+}-decontaminating materials[11,14−22,50] such as titanate nanofiber T3(H) (130.15 mg/g) and titanate nanofiber T3 (159.6 mg/g),[16] $Na_2Nb_2O_6{\cdot}H_2O$ (144.165 mg/g),[19] $K_4Nb_6O_{17}$ (205.95 mg/g),[18] and Na-4-mica (78.78 mg/g)[15] (Figure 2c). The comparisons of Ba^{2+} removal efficiencies by various sorbents in this work and references are listed in Table S18. The q_m^{Ni} is 83.27 ± 2.05 mg/g, and the q_m^{Co} is 51.98 ± 0.59 mg/g, both of which exceed those of many reported materials, such as kaolinite (10.4 mg/g for Ni^{2+} and 11.0 mg/g for Co^{2+}), montmorillonite (28.4 mg/g for Ni^{2+} and 28.6 mg/g for Co^{2+}), modified kaolinite (8.4 mg/g for Ni^{2+} and 9.0 mg/g for Co^{2+}), and modified montmorillonite (19.7 mg/g for Ni^{2+} and 22.3 mg/g for Co^{2+}).[33,37] The different capacities for Ba^{2+}, Ni^{2+}, and Co^{2+} may originate from the distinct hydrated radii of Ba^{2+} (4.04 Å), Ni^{2+} (4.04 Å), and Co^{2+} (4.23 Å).[56] The interlayer spaces of FJSM-SnS are large enough to load the full stoichiometric numbers of the hydrated Ba^{2+} and Ni^{2+} ions but not the larger hydrated Co^{2+} ions. Thus, the $[OAC]^+$ was completely exchanged by the Ba^{2+} and Ni^{2+} ions and partially exchanged by the Co^{2+} ions, which has been confirmed by the disappeared characteristic peak of nitrogen for Ba^{2+}- or Ni^{2+}-exchanged products and the subdued characteristic peak of nitrogen for the Co^{2+}-exchanged product in XPS spectra, respectively, (Figure S7g). Higher q_m^{Ba} is also attributed to some surface adsorption. Similar phenomena have also been found in other sulfide ion-exchangers.[42,44] The interlayer spaces of FJSM-SnS are large enough to load the full stoichiometric number of the hydrated form of Ni^{2+} ions but not the larger Co^{2+} ions. In addition, the fitting results give the b (L/mg) constants of 0.0237 ± 0.0072 for Ba^{2+}, 0.0225 ± 0.0025 for Ni^{2+}, and 0.061 ± 0.0044 for Co^{2+} (Table S4).

Kinetic Studies. In addition to the high capacity, the fast kinetics of the process further indicates that FJSM-SnS has outstanding removal efficiency. Specifically, over 94.6% of Ba^{2+} ions (initially ~370 μg/L), 99.0% of Ni^{2+} ions (initially ~1100 μg/L), and 98.8% of Co^{2+} ions (initially ~1000 μg/L) were removed within 5 min of contact (Figures S8−S10). The residual concentrations of Ba^{2+}, Ni^{2+}, and Co^{2+} within 5 min were 20.0, 10.94, and 12.2 μg/L (Tables S5−S7), respectively. The ion exchange kinetic data of Ba^{2+}, Ni^{2+}, and Co^{2+} were fitted with the pseudo-second-order kinetic model (eq S1).[57−60]

pH Dependent Ion-Exchange Studies and Irradiation. To further test the stability and functionality of FJSM-SnS, we performed the ion-exchange experiments under a wide range of pH conditions and found that FJSM-SnS retained its removal capacities for Ba^{2+} in pH = 3.3−10.8 and for Ni^{2+} and Co^{2+} in pH = 2.3−10.8. The removal efficiency R (eq S2) for Ba^{2+} can still reach 92.6% even at pH = 3.3. The distribution coefficient K_d (eq S3) for Ba^{2+} can range from 1.25 × 10^4 to 7.49 × 10^4 mL/g even in the conditions of 3.3 ≤ pH ≤ 8.1 (Figure 3a).

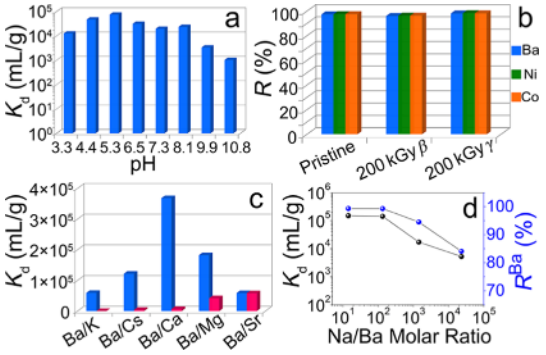

Figure 3. (a) Distribution coefficient (K_d) values of Ba^{2+} at various initial pH values; (b) removal efficiencies of Ba^{2+}, Ni^{2+}, and Co^{2+} using irradiated FJSM-SnS compared with pristine FJSM-SnS sample; (c) K_d^{Ba} values (blue) in the presence of excess alkali or alkaline-earth metal ions (red); and (d) variations of K_d^{Ba} (black) and R^{Ba} (blue) with the Na/Ba molar ratios.

Additionally, the K_d^{Ni} and K_d^{Co} values range from 2.62 × 10^2 to 8.92 × 10^4 mL/g and 4.67 × 10^2 to 3.75 × 10^5 mL/g in the conditions of 2.3 ≤ pH ≤ 10.8, respectively (Figure S12b). Importantly, the high K_d and R values were essentially unchanged even after 200 kGy β and γ irradiation as compared with the pristine unirradiated FJSM-SnS (Figure 3b, Table S10). The order of K_d for those three metal ions is Co^{2+} > Ba^{2+} > Ni^{2+} before and after 200 kGy β and γ irradiations, which is in agreement with the order of the corresponding constants b in the above equilibrium isotherms. The PXRD patterns reveal that the structure of FJSM-SnS was stable after ion-exchange for Ba^{2+} in pH = 3.3−10.8 and for Ni^{2+} and Co^{2+} in pH = 2.3−10.8 (Figures S11 and S12a) or using its corresponding samples after 200 kGy β and γ irradiations (Figure S13). Meanwhile, the ion-exchange experiments performed using the β and γ irradiated samples of FJSM-SnS suggest negligible leaching of Sn ions, indicating irradiation has no effect on FJSM-SnS (Table S10).

Competitive Ion-Exchange. The nuclear wastes typically contain excess of alkali or alkaline-earth metal ions, which can have a strong interference effect on the selective capture of targeted ions.[61−66] Hence, we investigated in more depth the selectivity of FJSM-SnS for Ba^{2+} in competitive experiments. For example, aiming at removing a concentration of 0.7 mg/L Ba^{2+} in the presence of individual excess of K^+, Cs^+, Ca^{2+}, Mg^{2+}, and Sr^{2+}, we find that FJSM-SnS retains high values of K_d^{Ba} from 5.84 × 10^4 to 3.68 × 10^5 mL/g (Figure 3c, Table S11). Particularly notable is the ultrahigh K_d^{Ba} value of 3.68 × 10^5 mL/g of FJSM-SnS under excess of competitive Ca^{2+} (Figure 3c, Table S11), representing 22-fold improvement over the highest K_d value for barium reported to date (1.60 × 10^4 mL/g of titanate nanofiber T3[16]). The ion-exchange ability of FJSM-SnS in the presence of excess Na^+ was also investigated. With tremendous excess of Na^+ (1437 fold), FJSM-SnS exhibited a removal rate R^{Ba} as high as 94.51% and K_d^{Ba} of 1.72

https://dx.doi.org/10.1021/acs.chemmater.9b04831
Chem. Mater. 2020, 32, 1957−1963

$\times 10^4$ mL/g. Even at the molar ratio (Na^+/Ba^{2+}) of 2.32×10^4, the uptake of Ba^{2+} still reached 84.08% (Figure 3d, Table S12).

We also investigated the performance of FJSM-SnS for Ba^{2+} selectivity in simulated groundwater. The solution was composed of four competitive cations, K^+, Na^+, Ca^{2+}, and Mg^{2+} with higher concentrations than that of Ba^{2+} (the initial Ba^{2+} concentration is 2.742 ppm) (Table S13). FJSM-SnS captured 85.93% of Ba^{2+}, and the residual Ba^{2+} concentration in the solution was 0.386 mg/L, that is, far below the EPA's 2 mg/L and WHO's 0.7 mg/L acceptable limits of drinking water.[6] Meanwhile, the general affinity order of FJSM-SnS in this simulated groundwater was $Ba^{2+} > Ca^{2+} > Mg^{2+} > Na^+ > K^+$, as revealed based on the K_d values of these ions (Table S13).

Because FJSM-SnS is an efficient ion-exchanger capturing Cs^+, Sr^{2+}, UO_2^{2+}, Eu^{3+}, Ba^{2+}, Ni^{2+}, and Co^{2+},[47−49] we also carried out the ion exchange experiments using the same concentrations or same moles of these ions to test the affinity order (Tables S14 and S15). Both the competitive experiments with the same concentrations and the same moles indicate that the order of the K_d values is $Eu^{3+} > Co^{2+} > Ba^{2+} > Sr^{2+} > Ni^{2+} > UO_2^{2+} > Cs^+$, which is different from the corresponding electronegativity order (Ni > Co > Eu > Sr > Ba > Cs). This trend indicates that not only electrostatics (or surface charge) but also a complex combination of factors including the soft S^{2-} ligands of FJSM-SnS, the hydration state of ions, and the hard/soft Lewis acid/base interactions with the cations plays a role in the capture kinetics.

Ion-Exchange Studies Using a Column. The above ion-exchange studies were based on the so-called batch (stirring) method. In many industrial and wastewater treatment processes, however, continuous bed flow ion-exchange columns are required. Here, the purification efficiency of FJSM-SnS for Ba^{2+}, Ni^{2+}, and Co^{2+} was tested using a fixed-bed ion-exchange column (Figure S1). It is noteworthy that the removal efficiency (R) can be maintained about 99% in low concentrations (704.9−928.6 μg/L) during processing 1100 bed volumes (bed volume = 2.80 mL) of mixture solution (Figure 4a). Moreover, after processing more than 3 L mixed solution, 99.74, 99.30, and 99.65% of Ba^{2+}, Ni^{2+}, and Co^{2+} could be removed, respectively. The residual concentrations were as low as 2.33 μg/L for Ba^{2+}, 6.24 μg/L for Ni^{2+}, and 3.25 μgL for Co^{2+} well under the environmental safety limits. This further demonstrates the effectiveness of FJSM-SnS for the removal of Ba^{2+}, Ni^{2+}, and Co^{2+} (Table S17). After the ion-exchange column experiments, the sorbent solids show deeper colors compared with the pristine compound consistent with the capture of Ba^{2+}, Ni^{2+}, and Co^{2+} ions (Figure 4b,c). In addition, the captured barium, nickel, and cobalt in the exchanged products can be easily recovered by eluting them with 0.5 M KCl solution (Figures S15−S18), which represents the first realization of reversible barium, nickel, and cobalt removal process for sulfide-based ion-exchangers to date.

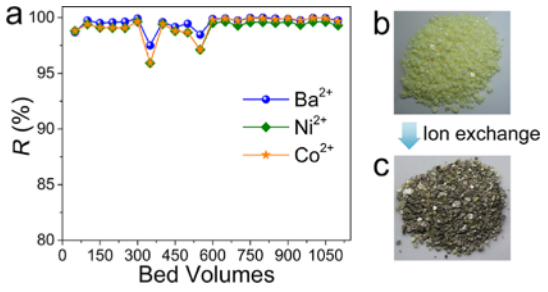

Figure 4. (a) Removal efficiencies of Ba^{2+}, Ni^{2+}, and Co^{2+} by FJSM-SnS plotted against bed volumes in the ion-exchange column experiments; photos of the pristine FJSM-SnS (b); and the product after column experiments with the coexisting Ba^{2+}, Ni^{2+}, and Co^{2+} (c).

CONCLUSIONS

In summary, the easy−to-synthesize layered metal sulfide FJSM-SnS is a very promising radioactive ion-exchanger that can operate over a relatively wide pH range. It not only exhibits extremely high sorption capability toward barium, nickel, and cobalt but also fast and efficient removal of barium ions in the presence of many competitive cations (K_d^{Ba} value as a new record). Moreover, FJSM-SnS has the advantages of good β and γ radiation resistance, acid resistance, and efficient elution of captured barium, nickel, and cobalt. The removal efficiency of FJSM-SnS toward barium, nickel, and cobalt is retained even after 200 kGy β and γ irradiation, which indicates its potential for application under harsh conditions in the remediation of radioactive contamination. The layered metal sulfide can be applied in ion exchange columns and achieve the capture of barium, nickel, and cobalt from complex wastewater. Therefore, the high capacities found in the sulfides can effectively reduce the volume of generated wastes here. This work underscores the enormous potential of metal sulfides as a new appealing low cost class of materials for high efficient and selective uptake of ^{133}Ba, ^{63}Ni, and ^{60}Co and their nonradioactive isotopes, as well as ^{226}Ra from complex wastewater.

ASSOCIATED CONTENT

Supporting Information

The Supporting Information is available free of charge at https://pubs.acs.org/doi/10.1021/acs.chemmater.9b04831.

Experimental section, PXRD, EDS, XPS, mapping, equations, tables for ion-exchange data and the stability study of FJSM-SnS (PDF)

AUTHOR INFORMATION

Corresponding Authors

Mei-Ling Feng − *State Key Laboratory of Structural Chemistry, Fujian Institute of Research on the Structure of Matter, Chinese Academy of Sciences, Fuzhou, Fujian 350002, P. R. China; Department of Chemistry, Northwestern University, Evanston, Illinois 60208, United States;* orcid.org/0000-0003-2524-0994; Email: fml@fjirsm.ac.cn

Mercouri G. Kanatzidis − *Department of Chemistry, Northwestern University, Evanston, Illinois 60208, United States;* orcid.org/0000-0003-2037-4168; Email: m-kanatzidis@northwestern.edu

Authors

Yu-Jie Gao − *State Key Laboratory of Structural Chemistry, Fujian Institute of Research on the Structure of Matter, Chinese Academy of Sciences, Fuzhou, Fujian 350002, P. R. China;* orcid.org/0000-0002-8216-1291

Hai-Yan Sun − *State Key Laboratory of Structural Chemistry, Fujian Institute of Research on the Structure of Matter, Chinese Academy of Sciences, Fuzhou, Fujian 350002, P. R. China*

https://dx.doi.org/10.1021/acs.chemmater.9b04831
Chem. Mater. 2020, 32, 1957−1963

Ji-Long Li − *State Key Laboratory of Structural Chemistry, Fujian Institute of Research on the Structure of Matter, Chinese Academy of Sciences, Fuzhou, Fujian 350002, P. R. China*
Xing-Hui Qi − *State Key Laboratory of Structural Chemistry, Fujian Institute of Research on the Structure of Matter, Chinese Academy of Sciences, Fuzhou, Fujian 350002, P. R. China*
Ke-Zhao Du − *State Key Laboratory of Structural Chemistry, Fujian Institute of Research on the Structure of Matter, Chinese Academy of Sciences, Fuzhou, Fujian 350002, P. R. China*
Yi-Yu Liao − *State Key Laboratory of Structural Chemistry, Fujian Institute of Research on the Structure of Matter, Chinese Academy of Sciences, Fuzhou, Fujian 350002, P. R. China; University of Chinese Academy of Sciences, Beijing 100049, P. R. China*
Xiao-Ying Huang − *State Key Laboratory of Structural Chemistry, Fujian Institute of Research on the Structure of Matter, Chinese Academy of Sciences, Fuzhou, Fujian 350002, P. R. China;* orcid.org/0000-0002-3514-216X

Complete contact information is available at: https://pubs.acs.org/10.1021/acs.chemmater.9b04831

Author Contributions

The manuscript was written through contributions of all authors. All authors have given approval to the final version of the manuscript.

Notes

The authors declare no competing financial interest.

■ ACKNOWLEDGMENTS

We thank the National Science Foundations of China (nos. 21771183 and 21521061), NSF of Fujian Province (no. 2018J01027), the FJIRSM&IUE Joint Research Fund (no. RHZX-2018-005). MGK thanks the National Science Foundation of the United States (grant DMR-1708254).

■ REFERENCES

(1) Beswick, A. J.; Gibb, F. G. F.; Travis, K. P. Deep borehole disposal of nuclear waste: engineering challenges. *Proc. Inst. Civ. Eng.: Energy* **2014**, *167*, 47−66.
(2) Cao, Q.; Huang, F.; Zhuang, Z.; Lin, Z. A study of the potential application of nano-$Mg(OH)_2$ in adsorbing low concentrations of uranyl tricarbonate from water. *Nanoscale* **2012**, *4*, 2423−2430.
(3) Hu, Q.-H.; Weng, J.-Q.; Wang, J.-S. Sources of anthropogenic radionuclides in the environment: a review. *J. Environ. Radioact.* **2010**, *101*, 426−437.
(4) Plecas, I.; Arbutina, D. Modelling of transport phenomena in concertr porous media. *J. Environ. Radioact.* **2013**, *14*, 1059−1065.
(5) Gad, H. M. H.; Lasheen, Y. F.; El-Zakla, T. S. Efficiency of locally prepared activated carbon in the preconcentration of barium-133 and radium-226 radionuclides in single and binary systems. *Radiochemistry* **2013**, *55*, 589−595.
(6) Shahwan, T.; Erten, H. N. Temperature effects in barium sorption on natural kaolinite and chlorite-illite clays. *J. Radioanal. Nucl. Chem.* **2004**, *260*, 43−48.
(7) Purdey, M. Chronic barium intoxication disrupts sulphated proteoglycan synthesis: a hypothesis for the origins of multiple sclerosis. *Med. Hypotheses* **2004**, *62*, 746−754.
(8) Wang, D.-Y.; Wang, Y. Phenotypic and behavioral defects caused by barium exposure in nematode Caenorhabditis elegans. *Arch. Environ. Contam. Toxicol.* **2008**, *54*, 447−453.
(9) Oliva, S. R.; Valdés, B.; Mingorance, M. D. Evaluation of some pollutant levels in bitter orange trees: Implications for human health. *Food Chem. Toxicol.* **2008**, *46*, 65−72.
(10) Ghaemi, A.; Torab-Mostaedi, M.; Ghannadi-Maragheh, M. Characterizations of strontium(II) and barium(II) adsorption from aqueous solutions using dolomite powder. *J. Hazard. Mater.* **2011**, *190*, 916−921.
(11) Chávez, M. L.; de Pablo, L.; García, T. A. Adsorption of Ba^{2+} by Ca-exchange clinoptilolite tuff and montmorillonite clay. *J. Hazard. Mater.* **2010**, *175*, 216−223.
(12) Fard, A. K.; McKay, G.; Chamoun, R.; Rhadfi, T.; Preud'Homme, H.; Atieh, M. A. Barium removal from synthetic natural and produced water using MXene as two dimensional (2-D) nanosheet adsorbent. *J. Radioanal. Nucl. Chem.* **2017**, *317*, 331−342.
(13) Edition, F. Guidelines for drinking-water quality. *WHO Chron.* **2011**, *38*, 104−108.
(14) Jurado-Vargas, M.; Oliguín, M. T.; Erdóñez-Regil, E.; Miménez-Reyes, M. Ion exchange of radium and barium in zeolites. *J. Radioanal. Nucl. Chem.* **1997**, *218*, 153−156.
(15) Komarneni, S.; Kozai, N.; Paulus, W. J. Superselective clay for radium uptake. *Nature* **2001**, *410*, 771.
(16) Yang, D. J.; Zheng, Z. F.; Zhu, H. Y.; Liu, H. W.; Gao, X. P. Titanate nanofibers as intelligent absorbents for the removal of radioactive ions from water. *Adv. Mater.* **2008**, *20*, 2777−2781.
(17) Seliman, A. F.; Lasheen, Y. F.; Youssief, M. A. E.; Abo-Aly, M. M.; Shehata, F. A. Removal of some radionuclides from contaminated solution using natural clay: bentonite. *J. Radioanal. Nucl. Chem.* **2014**, *300*, 969−979.
(18) Sun, J.; Yang, D.; Sun, C.; Liu, L.; Yang, S.; Jia, Y.; Cai, R.; Yao, X. Potassium niobate nanolamina: A promising adsorbent for entrapment of radioactive cations from water. *Sci. Rep.* **2014**, *4*, 7313.
(19) Sun, J.; Liu, L.; Zhao, X.; Yang, S.; Komarneni, S.; Yang, D. Capture of radioactive cations from water using niobate nanomaterials with layered and tunnel structures. *RSC Adv.* **2015**, *5*, 75354−75359.
(20) Araissi, M.; Ayed, I.; Elaloui, E.; Moussaoui, Y. Removal of barium and strontium from aqueous solution using zeolite 4A. *Water Sci. Technol.* **2016**, *73*, 1628−1636.
(21) Noli, F.; Kapnisti, M.; Buema, G.; Harja, M. Retention of barium and europium radionuclides from aqueous solutions on ash-based sorbents by application of radiochemical techniques. *Appl. Radiat. Isot.* **2016**, *116*, 102−109.
(22) Olguín, M. T.; Deng, S. Ce-Fe-modified zeolite-rich tuff to remove Ba^{2+}-like $^{226}Ra^{2+}$ in presence of As(V) and F^- from aqueous media as pollutants of drinking water. *J. Hazard. Mater.* **2016**, *302*, 341−350.
(23) Déjeant, A.; Bourva, L.; Sia, R.; Galoisy, L.; Calas, G.; Phrommavanh, V.; Descostes, M. Field analyses of U-238 and Ra-226 in two uranium mill tailings piles from Niger using portable HPGe detector. *J. Environ. Radioact.* **2014**, *137*, 105−112.
(24) Reinoso-Maset, E.; Ly, J. Study of uranium(VI) and radium(II) sorption at trace level on kaolinite using a multisite ion exchange model. *J. Environ. Radioact.* **2016**, *157*, 136−148.
(25) Hamed, M. M.; Holiel, M.; Ahmed, I. M. Sorption behavior of cesium, cobalt and europium radionuclides onto hydroxyl magnesium silicate. *Radiochim. Acta* **2016**, *104*, 873−890.
(26) Tsvetkov, G. O.; D'yachkov, A. B.; Gorkunov, A. A.; Labozin, A. V.; Mironov, S. M.; Firsov, V. A.; Panchenko, V. Y. Selective laser ionisation of radionuclide Ni-63. *Quantum Electron.* **2017**, *47*, 48−53.
(27) Mou, J.; Wang, G.; Shi, W.; Zhang, S. Impact of environmental conditions on the sorption behavior of radionuclide Ni-63(II) onto hierarchically structured gamma-MnO_2. *J. Radioanal. Nucl. Chem.* **2012**, *292*, 161−170.
(28) Baudin, J.; Adam, C.; Garnier-Laplace, J. Dietary uptake, retention and tissue distribution of Mn-54, Co-60 and Cs-137 in the rainbow trout (Oncorhynchus mykiss Walbaum). *Water Res.* **2000**, *34*, 2869−2878.
(29) Eyrolle, F.; Claval, D.; Gontier, G.; Antonelli, C. Radioactivity levels in major French rivers: summary of monitoring chronicles acquired over the past thirty years and current status. *J. Environ. Monit.* **2008**, *10*, 800−811.
(30) Liu, M.; Chen, C.; Hu, J.; Wu, X.; Wang, X. Synthesis of magnetite/graphene oxide composite and application for cobalt(II) removal. *J. Phys. Chem. C* **2011**, *115*, 25234−25240.

(31) Zhang, H.; Yu, X.; Chen, L.; Geng, J. Investigation of radionuclide Ni-63(II) sorption on ZSM-5 zeolite. *J. Radioanal. Nucl. Chem.* **2010**, *286*, 249−258.
(32) Forstner, U.; Wittman, G. T. W. *Metal Pollution in the Aquatic Environment*; Springer Verlag: Berlin, 1983.
(33) Bhattacharyya, K. G.; Sen Gupta, S. Calcined tetrabutylammonium kaolinite and montmorillonite and adsorption of Fe(II), Co(II) and Ni(II) from solution. *Appl. Clay Sci.* **2009**, *46*, 216−221.
(34) Li, J.; Wang, X.; Zhao, G.; Chen, C.; Chai, Z.; Alsaedi, A.; Hayat, T.; Wang, X. Metal-organic framework-based materials: superior adsorbents for the capture of toxic and radioactive metal ions. *Chem. Soc. Rev.* **2018**, *47*, 2322−2356.
(35) Zhang, B.; Li, W.-A.; Liao, Y.-Y.; Zhang, C.; Feng, M.-L.; Huang, X.-Y. $[CH_3NH_3]_4Ga_4SbS_9S_{0.28}O_{0.72}H$: A three-dimensionally open-framework heterometallic chalcogenidoantimonate exhibiting Ni^{2+} ion-exchange property. *Chem.—Asian J.* **2018**, *13*, 672−678.
(36) El-Nadi, Y. A. Solvent Extraction and its applications on ore processing and recovery of metals: classical approach. *Sep. Purif. Rev.* **2017**, *46*, 195−215.
(37) Bhattacharyya, K.; Sen Gupta, S. Kaolinite and montmorillonite as adsorbents for Fe(III), Co(II) and Ni(II) in aqueous medium. *Appl. Clay Sci.* **2008**, *41*, 1−9.
(38) Vengris, T.; Binkien, R.; Sveikauskait, A. Nickel, copper and zinc removal from waste water by a modified clay sorbent. *Appl. Clay Sci.* **2001**, *18*, 183−190.
(39) Hasar, H. Adsorption of nickel(II) from aqueous solution onto activated carbon prepared from almond husk. *J. Hazard. Mater.* **2003**, *97*, 49−57.
(40) Keränen, A.; Leiviskä, T.; Salakka, A.; Tanskanen, J. Removal of nickel and vanadium from ammoniacal industrial wastewater by ion exchange and adsorption on activated carbon. *Desalin. Water Treat.* **2015**, *53*, 2645−2654.
(41) Sylvester, P.; Milner, T.; Jensen, J. Radioactive liquid waste treatment at Fukushima Daiichi. *J. Chem. Technol. Biotechnol.* **2013**, *88*, 1592−1596.
(42) Mertz, J. L.; Fard, Z. H.; Malliakas, C. D.; Manos, M. J.; Kanatzidis, M. G. Selective removal of Cs^+, Sr^{2+}, and Ni^{2+} by $K_{2x}Mg_xSn_{3-x}S_6$ (x = 0.5-1) (KMS-2) relevant to nuclear waste remediation. *Chem. Mater.* **2013**, *25*, 2116−2127.
(43) Feng, M.-L.; Kong, D.-N.; Xie, Z.-L.; Huang, X.-Y. Three-dimensional chiral microporous germanium antimony sulfide with ion-exchange properties. *Angew. Chem., Int. Ed.* **2008**, *47*, 8623−8626.
(44) Sarma, D.; Islam, S. M.; Subrahmanyam, K. S.; Kanatzidis, M. G. Efficient and selective heavy metal sequestration from water by using layered sulfide $K_{2x}Sn_{4-x}S_{8-x}$ (x = 0.65-1; KTS-3). *J. Mater. Chem. A* **2016**, *4*, 16597−16605.
(45) Manos, M. J.; Kanatzidis, M. G. Metal sulfide ion exchangers: superior sorbents for the capture of toxic and nuclear waste-related metal ions. *Chem. Sci.* **2016**, *7*, 4804−4824.
(46) Yang, H.; Luo, M.; Luo, L.; Wang, H.; Hu, D.; Lin, J.; Wang, X.; Wang, Y.; Wang, S.; Bu, X.; Feng, P.; Wu, T. Highly selective and rapid uptake of radionuclide cesium based on robust zeolitic chalcogenide via stepwise ion-exchange strategy. *Chem. Mater.* **2016**, *28*, 8774−8780.
(47) Qi, X.-H.; Du, K.-Z.; Feng, M.-L.; Li, J.-R.; Du, C.-F.; Zhang, B.; Huang, X.-Y. A two-dimensionally microporous thiostannate with superior Cs^+ and Sr^{2+} ion-exchange property. *J. Mater. Chem. A* **2015**, *3*, 5665−5673.
(48) Feng, M.-L.; Sarma, D.; Qi, X.-H.; Du, K.-Z.; Huang, X.-Y.; Kanatzidis, M. G. Efficient removal 6and recovery of uranium by a layered organic-inorganic hybrid thiostannate. *J. Am. Chem. Soc.* **2016**, *138*, 12578−12585.
(49) Qi, X.-H.; Du, K.-Z.; Feng, M.-L.; Gao, Y.-J.; Huang, X.-Y.; Kanatzidis, M. G. Layered $(A)_2Sn_3S_7\bullet 1.25H_2O$ (A = organic cation) as efficient ion exchanger for rare earth element recovery. *J. Am. Chem. Soc.* **2017**, *139*, 4314−4317.
(50) Ding, N.; Kanatzidis, M. G. Permeable layers with large windows in $[(CH_3CH_2CH_2)_2NH_2]_5In_5Sb_6S_{19}\bullet 1.45H_2O$: High ion-exchange capacity, size discrimination, and selectivity for Cs ions. *Chem. Mater.* **2007**, *19*, 3867−3869.
(51) Ma, L.; Wang, Q.; Islam, S. M.; Liu, Y.; Ma, S.; Kanatzidis, M. G. Highly selective and efficient removal of heavy metals by layered double hydroxide intercalated with the MoS_4^{2-} ion. *J. Am. Chem. Soc.* **2016**, *138*, 2858−2866.
(52) Ma, S.; Fan, C.; Du, L.; Huang, G.; Yang, X.; Tang, W.; Makita, Y.; Ooi, K. Intercalation of macrocyclic crown ether into well-crystallized LDH: Formation of staging structure and secondary host-guest reaction. *Chem. Mater.* **2009**, *21*, 3602−3610.
(53) Ma, S.; Chen, Q.; Li, H.; Wang, P.; Islam, S. M.; Gu, Q.; Yang, X.; Kanatzidis, M. G. Highly selective and efficient heavy metal capture with polysulfide intercalated layered double hydroxides. *J. Mater. Chem. A* **2014**, *2*, 10280−10289.
(54) Tudorache, A.; Marin, C.; Ioniţă, D. E.; Badea, I. A. Assessing barium and strontium concentrations and speciation in groundwater from the area of the future weak and medium radioactive waste repository Saligny-Romania. *Carpath. J. Earth Environ.* **2018**, *13*, 57−66.
(55) Do, D. D. *Adsorption Analysis: Equilibria and Kinetics*; Imperial College Press: London, 1998.
(56) Nightingale, E. R. Phenomenological theory of ion solvation effective radii of hydrated ions. *J. Phys. Chem.* **1959**, *63*, 1381−1387.
(57) Rudzinski, W.; Plazinski, W. Studies of the kinetics of solute adsorption at solid/solution interfaces: On the possibility of distinguishing between the diffusional and the surface reaction kinetic models by studying the pseudo-first-order kinetics. *J. Phys. Chem. C* **2007**, *111*, 15100−15110.
(58) Ho, Y.; McKay, G. The kinetics of sorption of divalent metal ions onto sphagnum moss peat. *Water Res.* **2000**, *34*, 735−742.
(59) Ho, Y. S.; McKay, G. Pseudo-second order model for sorption processes. *Process Biochem.* **1999**, *34*, 451−465.
(60) Wang, Z.; Giammar, D. E. Tackling deficiencies in the presentation and interpretation of adsorption results for new materials. *Environ. Sci. Technol.* **2019**, *53*, 5543−5544.
(61) Riley, B. J.; Chun, J.; Um, W.; Lepry, W. C.; Matyas, J.; Olszta, M. J.; Li, X.; Polychronopoulou, K.; Kanatzidis, M. G. Chalcogen-based aerogels as sorbents for radionuclide remediation. *Environ. Sci. Technol.* **2013**, *47*, 7540−7547.
(62) Fan, Q. H.; Tan, X. L.; Li, J. X.; Wang, X. K.; Wu, W. S.; Montavon, G. Sorption of Eu(III) on attapulgite studied by batch, XPS, and EXAFS techniques. *Environ. Sci. Technol.* **2009**, *43*, 5776−5782.
(63) Standring, W. J. F.; Oughton, D. H.; Salbu, B. Potential remobilization of ^{137}Cs, ^{60}Co, ^{99}Tc and ^{90}Sr from contaminated Mayak sediments river and estuary environments. *Environ. Sci. Technol.* **2002**, *36*, 2330−2337.
(64) Zhu, L.; Xiao, C.; Dai, X.; Li, J.; Gui, D.; Sheng, D.; Chen, L.; Zhou, R.; Chai, Z.; Albrecht-Schmitt, T. E.; Wang, S. Exceptional perrhenate/pertechnetate uptake and subsequent immobilization by a low-dimensional cationic coordination polymer: overcoming the hofmeister bias selectivity. *Environ. Sci. Technol. Lett.* **2017**, *4*, 316−322.
(65) Mei, L.; Li, F. Z.; Lan, J. H.; Wang, C. Z.; Xu, C.; Deng, H.; Wu, Q. Y.; Hu, K. Q.; Wang, L.; Chai, Z. F.; Chen, J.; Gibson, J. K.; Shi, W. Q. Anion-adaptive crystalline cationic material for $^{99}TcO_4^-$ trapping. *Nat. Commun.* **2019**, *10*, 1532.
(66) Zhang, J.; Chen, L.; Dai, X.; Zhu, L.; Xiao, C.; Xu, L.; Zhang, Z.; Alekseev, E. V.; Wang, Y.; Zhang, C.; Zhang, H.; Wang, Y.; Diwu, J.; Chai, Z.; Wang, S. Distinctive two-step intercalation of Sr^{2+} into a coordination polymer with record high Sr-90 uptake capabilities. *Chem* **2019**, *5*, 977−994.

https://dx.doi.org/10.1021/acs.chemmater.9b04831
Chem. Mater. 2020, 32, 1957−1963